Adsorption (2007) 13: 247–256
DOI 10.1007/s10450-007-9068-7

Preparation of MCM-41 silica using the cationic surfactant blend

Arnošt Zukal · Helena Šiklová · Jiří Čejka · Matthias Thommes

Received: 6 April 2007 / Revised: 29 September 2007 / Accepted: 8 October 2007 / Published online: 23 October 2007

Abstract A series of samples of MCM-41 silica was synthesized using surfactant blends of 1-alkyl-3-methylimidazolium and alkyltrimethylammonium salts or blends of two different 1-alkyl-3-methylimidazolium salts (alkyl denotes octyl or hexadecyl) as structure-directing agents. The precipitation of solid particles from a homogeneous water solution of sodium metasilicate and surfactant blend was achieved by lowering the pH due to the hydrolysis of ethyl acetate added. The molecular sieves were characterized by scanning as well as transmission electron microscopy, X-ray powder diffraction, and nitrogen adsorption using a proper nonlocal density functional theory approach for calculations of the textural parameters. All the prepared silicas were of MCM-41-type; they differ in the integral breadth of the pore size distribution curve and the presence of secondary mesopores. The best quality MCM-41 silica of spherical particle morphology was synthesized by using of optimized blend of hexadecyltrimethylammonium bromide and 1-methyl-3-octylimidazolium chloride. The results obtained showed that spherical particles are composed of domains of perfectly ordered hexagonal porous structure. Some samples prepared by using 1-alkyl-3-methylimidazolium salts featured a narrow pore size distribution. However, they contained a small volume of secondary mesopores.

A. Zukal (✉) · H. Šiklová · J. Čejka
J. Heyrovský Institute of Physical Chemistry, v.v.i., Academy of Sciences of the Czech Republic, Dolejškova 3, 182 23 Prague 8, Czech Republic
e-mail: arnost.zukal@jh-inst.cas.cz

M. Thommes
Quantachrome Instruments, 1900 Corporate Drive, Boynton Beach, Florida 33426, USA

Keywords Mesoporous molecular sieves · Synthesis and characterization · Nitrogen adsorption isotherms

Abbreviations

S_{BET}	BET surface area, m^2/g
S_{ME}	cumulative mesopore area, m^2/g
V_{ME}	cumulative mesopore volume, cm^3/g
D_{ME}	mesopore mode diameter, nm
ΔD_{ME}	integral breadth of the mesopore distribution curve, nm
V_{SEC}	volume of secondary mesopores, cm^3/g
V_{TOT}	total pore volume, cm^3/g
W_{ME}	mesopore size calculated using equation (1), nm

1 Introduction

The air and moisture stable room-temperature ionic liquids (RTIL) have currently received considerable attention as novel media for chemical synthesis (Wasserscheid and Welton 2003), homogeneous catalysis (Gordon 2001), electrochemistry (Lagrost et al. 2003), and separation techniques (Scurto et al. 2003). Their unique properties offer a great potential for many applications as nonvolatile, nonflammable, environmentally benign alternatives to conventional organic solvents (Welton 1999; Wasserscheid and Keim 2000; Miskolczy et al. 2004). Ionic liquids with imidazole heads, such as 1-alkyl-3-methylimidazolium salts, possess a positively charged hydrophilic ring with a hydrophobic organic chain of different length. Thus, they are one category of cationic surfactants and provide the way to prepare nanostructured solids, either with tailored nanoporous structure or with defined particle morphology (Antonietti et al. 2004).

The communication (Adams et al. 2001) describes the first synthesis of mesoporous silica by using the 1-hexadecyl-3-methylimidazolium chloride. The mesoporous structure of this material was similar to the structure of MCM-41; however, it was not as regular as mesoporous structure of well ordered MCM-41 samples. Several recent reports have focused on the utilization of various RTILs as structure-directing agents (SDA) for the synthesis of mesoporous silica materials. A series of mesoporous silica nanoparticles with various porous structures was synthesized from mild basic solution employing 1-C_nH_{n+1}-3-methylimidazolium bromide (where n = 14, 16 or 18) or 1-tetradecyl-oxymethyl-3-methylimidazolium chloride as SDA (Trewyn et al. 2004). Monolithic mesoporous silica with either wormlike pores or lamellar structure have been prepared by using 1-butyl-3-methylimidazolium tetrafluoroborate or 1-C_nH_{n+1}-3-methylimidazolium chloride (where n = 10, 14, 16 or 18), respectively (Zhou and Antonietti 2003, 2004; Zhou et al. 2004). Imidazole type RTILs, 1-hexadecyl-3-methylimidazolium chloride and 1-hexadecyl-3-methylimidazolium ruthenium hexachloride, have been used to fabricate the well-ordered hexagonal mesoporous silica and Ru-SiO_2, respectively (Zhu et al. 2006). 1-Hexadecyl-3-methylimidazolium chloride has been also used as a template to prepare mesoporous silica with cubic (MCM-48-type) and hexagonal (MCM-41-type) frameworks (Wang et al. 2007). This RTIL structure director showed a broad range of conditions allowing the synthesis of cubic mesostructures with improved reproducibility.

RTILs were used as SDA not only for the preparation of siliceous materials but also in the synthesis of mesoporous alumina as demonstrated recently (Žilková et al. 2006). The alumina prepared using 1-octyl-3-methylimidazolium chloride as SDA was characterized by a wormhole framework structure and a narrow pore size distribution.

The syntheses of mesoporous silica or alumina based on the use of RTIL as the SDA were accomplished with pure RTILs until now. However, surfactants blends offer new possibilities in the design of mesoporous materials as their structure and morphology can be controlled through the choice of two surfactants with different properties and the adjustment of composition. Soon after the discovery of templated mesoporous materials (Kresge et al. 1992), hexadecylpyridinium chloride surfactant in combination with hexadecyltrimethylammonium chloride was employed (Khushalani et al. 1996). This surfactant system led to MCM-41 materials with tunable pore diameter. Using a mixture of hexadecyltrimethylammonium bromide and sodium carboxylate (sodium laurate) siliceous MCM-48 molecular sieve has been synthesized (Chen et al. 1997, 1998). MCM-41 silica with spherical particles was prepared by using of the optimized blend of cetyltrimethylammonium bromide and 1-methyl-3-octylimidazolium chloride (Zukal et al. 2007). In the following study, an in-depth report on the use of mixed alkyltrimethylammonium halides with different carbon chain lengths to synthesize MCM-41 was presented (Cheng et al. 1999). The mixed surfactant systems have demonstrated the possibility of tuning of nanometer-scale structure and micrometer-scale morphology by adjusting the mixing ratio of the mixed surfactant system. Highly-ordered MCM-41 silica with various pore diameters has been obtained when micelle packing was suitably controlled with a mixture of alkyltrimethylammonium bromide and alkyltriethylammonium bromide according to the length of C_{12}-C_{22} alkyl groups (Ryoo et al. 1999a). The mixture of alkyltrimethyl ammonium bromide and polyoxyethylene/alkyl/ether surfactants has facilitated the synthesis of MCM-48 silica (Ryoo et al. 1999b). High-quality mesoporous silica materials with hexagonal and cubic structures have been synthesized by using blends of nonionic diblock and Pluronic triblock amphiphilic block copolymers as the SDA (Kim et al. 2002). SBA-16 mesoporous silicas have been synthesized using Pluronic F127 poly(ethylene oxide)-poly(propylene oxide)-poly(ethylene oxide) triblock copolymer ($EO_{106}PO_{70}EO_{106}$) and its blends with Pluronic P123 ($EO_{20}PO_{70}EO_{20}$) as structure directors (Kim et al. 2004).

We have developed a general procedure for the synthesis of templated mesoporous silicas, which is based on the precipitation of the solid product from a homogeneous water solution of sodium metasilicate and a suitable cationic or nonionic surfactant (Rathouský and Zukal 2003; Rathouský et al. 2004). The decrease in the pH of the reaction mixture, which induces the formation of solid particles, was achieved by the controlled hydrolysis of acetic acid ethyl ester. In the present study, the developed synthesis route has been adapted for the preparation of templated mesoporous silica using the blends of 1-alkyl-3-methylimidazolium and alkyltrimethylammonium salts or blends of two different 1-alkyl-3-methylimidazolium salts (alkyl denotes octyl or hexadecyl).

2 Experimental

2.1 Chemicals

1-Hexadecyl-3-methylimidazolium chloride (C_{16}MIMCl) was purchased by Merck. 1-Octyl-3-methylimidazolium chloride (C_8MIMCl), octyltrimetylammonium bromide (C_8TMABr), hexadecyltrimetylammonium bromide (C_{16}TMABr) and sodium metasilicate (Na_2SiO_3) were purchased by Aldrich. Ethyl acetate was obtained from Fluka.

Table 1 Molar compositions of reaction mixtures

Sample code	Na_2SiO_3	C_8MIMCl	C_{16}MIMCl	C_8TMABr	C_{16}TMABr	H_2O
A1	1	0.529	–	–	0	1524
A2	1	0.397	–	–	0.084	1524
A3	1	0.265	–	–	0.167	1524
A4	1	0.132	–	–	0.251	1524
A5	1	0	–	–	0.335	1524
B1	1	–	0.356	0	–	1524
B2	1	–	0.267	0.121	–	1524
B3	1	–	0.178	0.242	–	1524
B4	1	–	0.089	0.363	–	1524
B5	1	–	0	0.968	–	1524
C1	1	–	0.267	–	0.084	1524
C2	1	–	0.178	–	0.167	1524
C3	1	–	0.089	–	0.251	1524
D1	1	0.397	0.089	–	–	1524
D2	1	0.265	0.178	–	–	1524
D3	1	0.132	0.267	–	–	1524

2.2 Synthesis

The reaction mixture was prepared in an autoclavable Nalgene bottle at the temperature of 35 °C. In the typical synthesis, m g of 1-alkyl-3-methylimidazolium chloride and $(4 - m)$ g of alkyltrimethylammonium bromide (or 4 g of the pure surfactant) followed by 4 g of Na_2SiO_3 were dissolved in 900 ml of distilled water at 35 °C, resulting in the formation of a clear solution. Afterwards 5 ml of ethyl acetate was quickly added, the mixture was stirred for 1 min and the stirring was stopped. After 5–10 min a precipitate began to form and the mixture was allowed to stand at 35 °C for 5 h. During this period the precipitation of solid particles from the solution by sedimentation occurred. The suspension of the solid product in the mother liquor was kept at 95 °C for 48 h in a heating box. During the ageing, organic vapor was allowed to escape through leaks in the cap of the bottle.

The resulting solid was recovered by filtration, extensively washed out with distilled water and ethanol, and dried at ambient temperature. The templates were removed by calcination in air at 540 °C for 8 h (temperature ramp of 1 °C/min).

The sample codes and the molar composition of the reaction mixtures are listed in Table 1. The compositions of the reaction mixtures given in this table show that the samples of series A were prepared using the blends C_8MIMCl and C_{16}TMABr. In the series B, C, and D the blends of C_{16}MIMCl and C_8TMABr, C_{16}MIMCl and C_{16}TMABr or C_8MIMCl and C_{16}MIMCl, respectively, were investigated as the SDA. As the blends of different alkyltrimethylammonium halides as the SDA were investigated in detail (Cheng et al. 1999), they were omitted in this study.

2.3 SEM, TEM, XRD, and nitrogen adsorption characterizations

X-ray powder diffraction data were recorded on a Bruker D8 X-ray powder diffractometer equipped with a graphite monochromator and position sensitive detector (Våntec-1) using CuKα radiation (at 40 kV and 30 mA) in Bragg-Brentano geometry.

The size and shape of synthesized particles were evaluated by scanning electron microscopy images using a JEOL JSM-5500LV instrument.

High-resolution transmission electron microscopy (HRTEM) images were obtained with a JEOL JEM-3010 instrument operating at an accelerating voltage 300 kV using LaB6 cathode and resolution 0.17 nm. The samples were ultrasonically dispersed in ethanol and then dropped onto the carbon-coated copper grids prior to the measurements.

Nitrogen (purity 99.999 vol.%) supplied by Messer (Griesheim, Germany) was used as adsorptive. Sorption isotherms of nitrogen at −196 °C (i.e. 77.35 K) on silicas under study were determined using a conventional static volumetric technique. In order to attain a sufficient accuracy

in the accumulation of the adsorption data, this instrument is equipped with pressure transducers covering the 133 Pa, 1.33 kPa and 133 kPa ranges.

Before each sorption measurement the sample was outgassed using a special heating program allowing for a slow removal of most preadsorbed water at low temperatures. This was done to avoid potential structural damage of the sample due to surface tension effects and hydrothermal alternation. Starting at ambient temperature the sample was outgassed at 110 °C (temperature ramp of 0.5 °C/min) until the residual pressure of 0.5 Pa was obtained. After further heating at 110 °C for 1 h the temperature was increased (temperature ramp of 1 °C/min) until the temperature of 250 °C was achieved. This temperature was maintained for 8 h.

2.4 Nonlocal density functional theory (NLDFT) method for pore size characterization

The adsorption data were analyzed using an advanced NLDFT approach dedicated to the system N_2 (77.35 K)/cylindrical silica pores. The advantage of the NLDFT method compared with the classical methods is that it allows calculating of the pore size distribution over the complete micro- and mesopore range. Here we apply a novel approach which allows to calculate the pore size distribution from the adsorption branch, i.e. in the region of hysteresis the method takes correctly into account the effect of delayed pore condensation (the kernel of metastable adsorption isotherms is applied), while the method uses in the region of reversible adsorption/desorption the kernel of NLDFT equilibrium isotherms. Details of this NLDFR method are described elsewhere (Neimark and Ravikovitch 2001; Ravikovitch and Neimark 2001; Lowell et al. 2004).

3 Results and discussion

3.1 Nitrogen adsorption and XRD investigations

Nitrogen isotherms recorded at −196 °C on the samples of the series A prepared using the blends of C_8MIMCl and C_{16}TMABr as the SDA are shown in Fig. 1. The isotherm on the sample A1, prepared with pure C_8MIMCl, is typical for silica templated with surfactant with a short hydrocarbon chain. The isotherms on further samples are characterized by the sudden increase in the amount adsorbed in the range of relative pressures p/p_0 of 0.35–0.40 as a result of the volume filling of MCM-41 mesopores. In the region of $p/p_0 > 0.4$ the nitrogen amount adsorbed on samples A1 and A2 depends on the relative pressure only very slightly; both isotherms are fully reversible. This fact clearly indicates that these samples do not contain any additional mesoporosity. The nitrogen isotherms on silicas A3 and A4

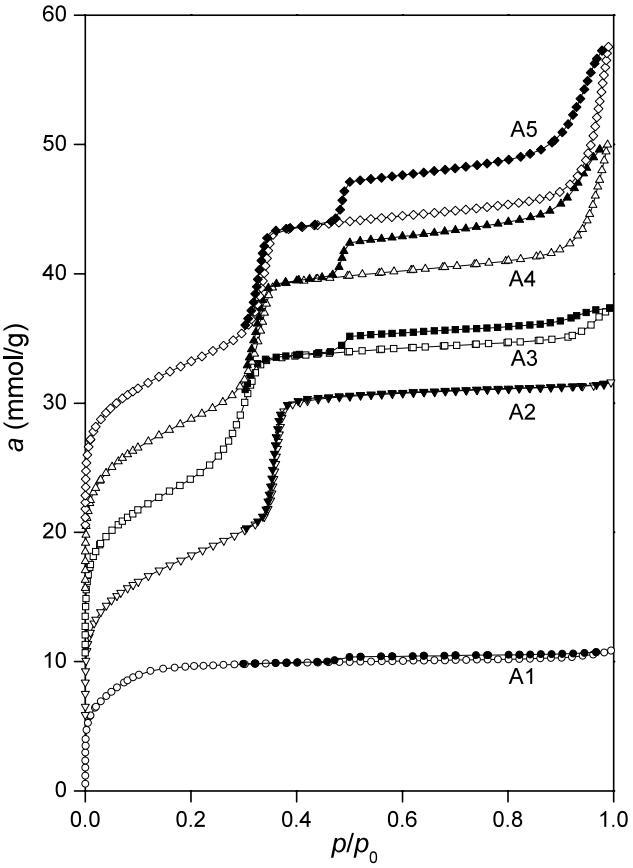

Fig. 1 Nitrogen isotherms on samples of series A at −196 °C. Except of that on sample A1, isotherms are shifted by 5 mmol/g each. *Solid symbols* denote desorption

prepared with surfactant blends containing larger amount of CTMABr and on silica A5 prepared with pure CTMABr are characterized by pronounced hysteresis loops in the region of $p/p_0 > 0.4$. The existence of this loop evidences the presence of secondary mesoporosity, i.e. structural defect holes in the MCM-41 particles (Lin et al. 2000).

The structural parameters of the samples of the series A are listed in Table 2. The BET surface areas were calculated using data in a relative pressure range from 0.05 to 0.25. The characteristics of MCM-41 mesoporous structure were obtained by NLDFT analysis of nitrogen isotherms in the region of $p/p_0 < 0.5$. The NLDFT pore size distribution curves are shown in Fig. 2. The presence of a single maximum evidences that all samples do not contain any microporosity. The cumulative mesopore area S_{ME}, cumulative mesopore volume V_{ME} and mesopore mode diameter D_{ME} are given in Table 2. The value of ΔD_{ME} in this table indicates the integral breadth of mesopore size distribution curve, defined as the width of a rectangle having the same area and height.

The pore size distribution of secondary mesopores was assessed from the adsorption branch of the nitrogen isotherm

Table 2 Structural parameters

Sample code	S_{BET} m^2/g	S_{ME} m^2/g	V_{ME} cm^3/g	D_{ME} nm	ΔD_{ME} nm	W_{ME} nm	V_{SEC} cm^3/g	V_{TOT} cm^3/g
A1	714	743	0.34	2.10	0.39	–	–	0.35
A2	951	899	0.90	4.05	0.29	4.04	–	0.92
A3	1175	947	0.84	3.63	0.42	3.55	0.20	1.04
A4	1125	927	0.87	3.79	0.38	3.71	0.53	1.37
A5	1076	891	0.85	3.86	0.35	3.77	0.67	1.59
B1	1054	881	0.85	3.90	0.29	3.90	0.30	1.16
B2	1094	902	0.85	3.80	0.35	3.87	0.41	1.26
B3	1031	866	0.82	3.85	0.32	3.92	0.38	1.20
B4	1053	876	0.84	3.83	0.41	3.91	0.11	0.95
B5	700	724	0.31	1.98	0.36	–	0.18	0.50
C1	1043	867	0.82	3.75	0.32	3.87	0.34	1.17
C2	1076	888	0.82	3.71	0.34	3.80	0.35	1.18
C3	1095	896	0.83	3.73	0.35	3.73	0.51	1.34
D1	1023	856	0.83	3.86	0.37	3.95	–	0.83
D2	1034	866	0.82	3.81	0.32	3.91	0.38	1.20
D3	1047	877	0.85	3.92	0.30	3.97	0.27	1.13

S_{BET}, BET surface area; S_{ME}, cumulative mesopore area; V_{ME}, cumulative mesopore volume; D_{ME}, mesopore mode diameter; ΔD_{ME}, integral breadth of the mesopore distribution curve; W_{ME}, mesopore size calculated using (1); V_{SEC}, volume of secondary mesopores; V_{TOT}, total pore volume

using the NLDFT approach. With the samples A3, A4, and A5 the secondary mesoporosity is characterized by the wide pore size distribution between 20 and 50 nm. The volume of secondary mesopores V_{SEC} and the total pore volume V_{TOT} determined from the amount adsorbed at a relative pressure of about 0.99 are provided in Table 2.

X-ray diffraction patterns of samples of the series A are presented in Fig. 3. It can be seen that the sample A2 features the best ordered mesoporous structure; the enlarged X-ray pattern exhibits six narrow peaks typical for the hexagonal ordering of the porous framework (see inset in Fig. 3).

On the basis of combination of adsorption and XRD data the size of mesopores was calculated. For the infinite structure of uniform cylindrical pores arranged in a hexagonal pattern with the (100) interplanar spacing d, the pore size W_{ME} can be expressed as

$$W_{ME} = cd[\rho V_{ME}/(1 + \rho V_{ME})]^{1/2}, \quad (1)$$

where ρ is the density of walls of the samples ($\rho = 2.2$ g/cm^3) and $c = [8/(3^{1/2}\pi)]^{1/2} = 1.213$ is a constant (Kruk et al. 1997). One can notice that calculated values of W_{ME} (Table 2) are in a good agreement with the mode pore diameter D_{ME} obtained by NLDFT approach.

The inspection of the results obtained on the samples of the series A clearly reveals that structural parameters of the sample A2 correspond to those of the best quality MCM-41. The integral breadth of the distribution of primary mesopores of the sample A2 has the minimum; moreover, this sample does not contain micropores or secondary mesopores. The breadth of mesopore distribution and presence of secondary mesopores show that other samples of the series A are of the worse quality. This fact is supported by the corresponding X-ray diffraction patterns (Fig. 3).

The nitrogen adsorption isotherms on the samples of series B, C, and D are similar to those on the samples A4 or A5; thus, it appears that the all samples are of MCM-41 type with more or somewhat less ordered mesoporous structure and some volume of secondary mesopores. The XRD patterns and the nitrogen isotherms for samples of series B, C, and D were processed by the same procedure as the samples of series A. The structural parameters (Table 2) revealed that these samples are characterized by a high surface area and a mesopore volume typical for MCM-41 silica. However, the samples of the series B, C, and D differ in the integral breadth of mesopore size distribution curve. The nitrogen isotherms on the best samples B1 and D3 from these series are shown in Fig. 4. Apart from the fact that samples B1

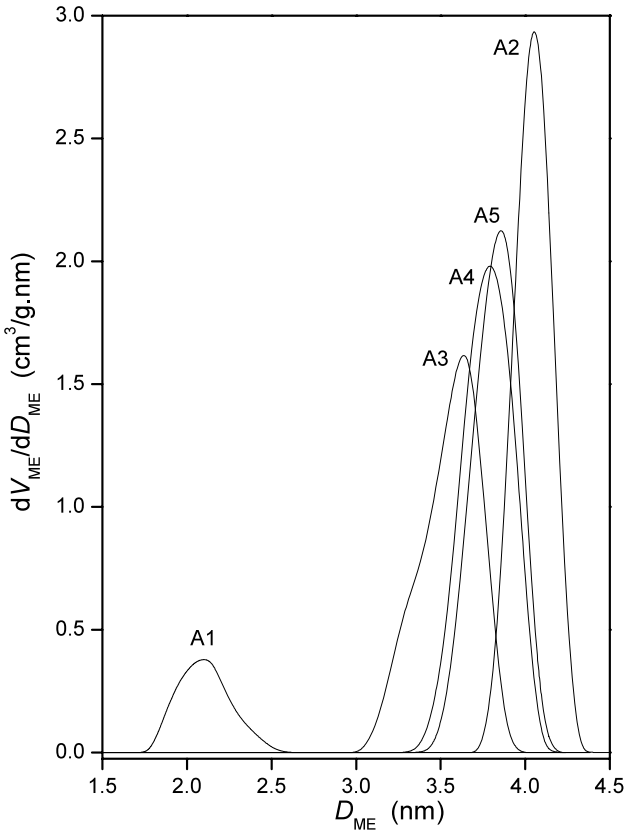

Fig. 2 NLDFT pore size distribution curves of samples of series A

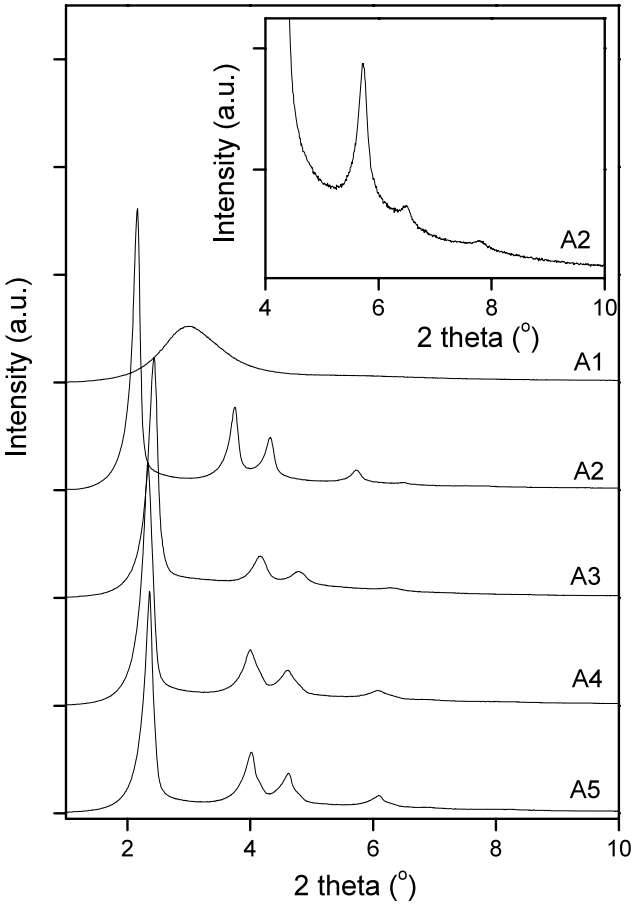

Fig. 3 XRD patterns of samples of series A. The *inset* shows enlarged pattern of the sample A2

and D3 contain some amount of secondary mesopores, the integral breadth of the mesopore size distribution (Fig. 5) attains a value of 0.29 or 0.30, respectively. The character of the well-ordered mesopore structure of the sample B1 and D3 is confirmed by X-ray diffraction patterns (Fig. 6).

3.2 SEM and HRTEM investigations

The HRTEM images of the sample A2 are presented in Figs. 7 and 8. Figure 7 evidences that the particles of MCM-41 are composed of perfectly ordered hexagonal structure while Fig. 8 shows that the mesopores are oriented from the external surface of the particle towards its center. This was confirmed on a number of different particles investigated and prepared in different synthesis batches, which evidences not only very good reproducibility of this synthetic method but also very good ordering of all spherical particles. However, the HRTEM images show only microscopic part of the spherical particle. As shown in the foregoing paragraph, the overall view of the structure ordering of a macroscopic amount of the sample obtained by means of XRD indicates excellent structural uniformity of the material.

SEM investigation of the prepared materials revealed that the sample A2 is characterized by the regular particle morphology while the particle shape and size of other samples are rather irregular. The SEM image in Fig. 9 evidences that the sample A2 is composed of spherical particles with diameters lying between 1.8 and 2.2 μm. The SEM image of the sample B1 is shown in Fig. 10, which is also characterized by the well-ordered MCM-41 mesoporous structure and the presence of secondary mesopores. It appears that irregular particles with a diameter of approximately 3–4 μm are agglomerates of smaller particles; the voids among them obviously create the secondary mesoporous structure observed in nitrogen adsorption isotherm.

The SEM investigation of the sample D3 provided the same results as that of the sample B1.

3.3 Formation of MCM-41 particles

In many cases, two different surfactants are completely miscible and exhibit complex phase behaviors in aqueous solutions. The phase behavior of mesoporous structures is determined by a packing factor

$$g = V/a_0 L, \tag{2}$$

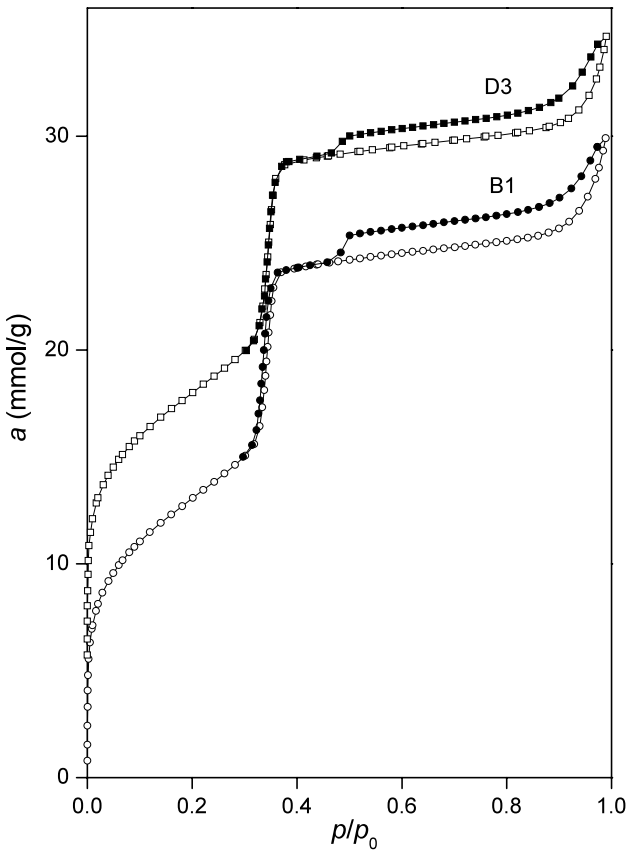

Fig. 4 Nitrogen isotherms on samples B1 and D3 at −196 °C. The isotherm on sample D3 is shifted by 5 mmol/g. *Solid symbols* denote desorption

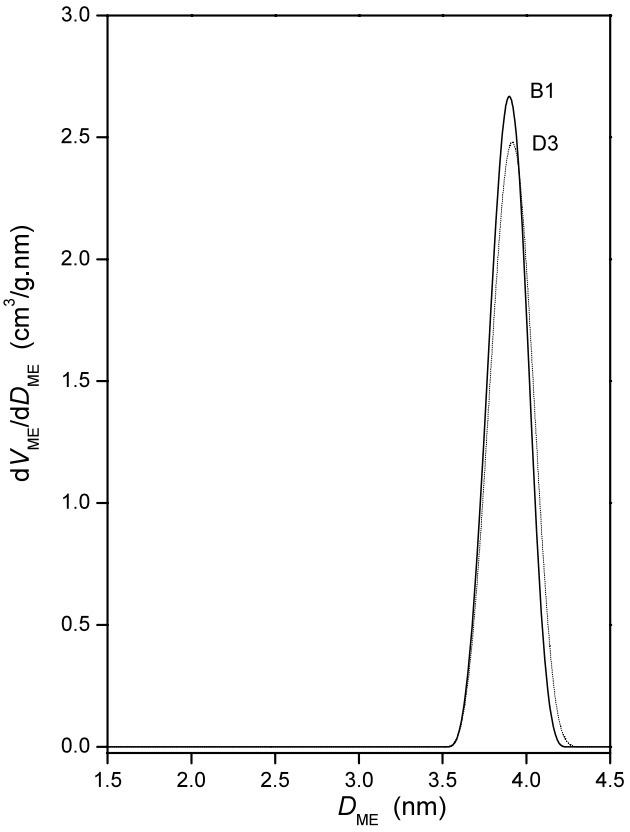

Fig. 5 NLDFT pore size distribution curves of samples B1 and D3

where V is the volume of surfactant chain, a_0 is the effective head area at the micelle surface and L is the kinetic surfactant chain length. The mesophase structure can be controlled by adjusting the g factor, i.e. by adjusting $g \cong 1/2$ for hexagonal $p6m$ phase (Roth and Vartuli 2005).

RTILs with planar aromatic imidazole head group have a unique a_0 value as compared with bulky three-dimensional head group of alkyltrimethylammonium surfactants. In mixed surfactant systems the g factor can be changed continuously by varying the ratio of the surfactants species involved. The present synthesis system consists of sodium metasilicate, alkyltrimethylammonium bromide, and the 1-alkyl-3-methylimidazolium chloride dissolved in basic solution. The obtained results show that the sample A2 is made of the MCM-41 porous framework and that there is no amorphous component. It means that the used combination of C_8MIMCl with a short alkyl chain and CTMABr with a long alkyl chain has enabled us to adjust the packing of micelles into the optimum cylindrical form corresponding to $g = 1/2$.

According to the charge-density-match theory, three close coupled phenomena can be identified as crucial ones for the formation of surfactant-silicate mesophases (Monnier et al. 1993). These include: (*i*) the binding of monomeric silicates and multidentate binding of silicate oligomers, (*ii*) preferred polymerization of silicates at the surfactant-silicate interface, and (*iii*) charge density matching across the interface. Multidentate ionic binding in the surfactant-silicate system has an important consequence; namely, it leads to precipitation of a given mesophase from solution. Through the interactions driving the precipitation process, the appearance of a given mesostructure is established, although this process is expected to operate on a different time scale from polymerization of the silica.

The synthesis of the sample A2 was performed using the blend of C_8MIMCl and C_{16}TMABr; the samples B1 or D3 were prepared using only 1-alkyl-3-methylimidazolium chlorides. Therefore, the charge density on the micelle surface, which was composed of either a mixture of alkylammonium and 1-alkyl-3-methylimidazolium head groups or only 1-alkyl-3-methylimidazolium head groups, was different. As the silicate anions in the solution are strongly attracted by the electrostatic interaction with the positively charged head groups of the micelles, the difference in the charge density can influence the formation of particles. The SEM investigation permits us to propose formation mechanism for sample B1 and D3. In the early stages of homogeneous precipitation the formation of small rigid particles

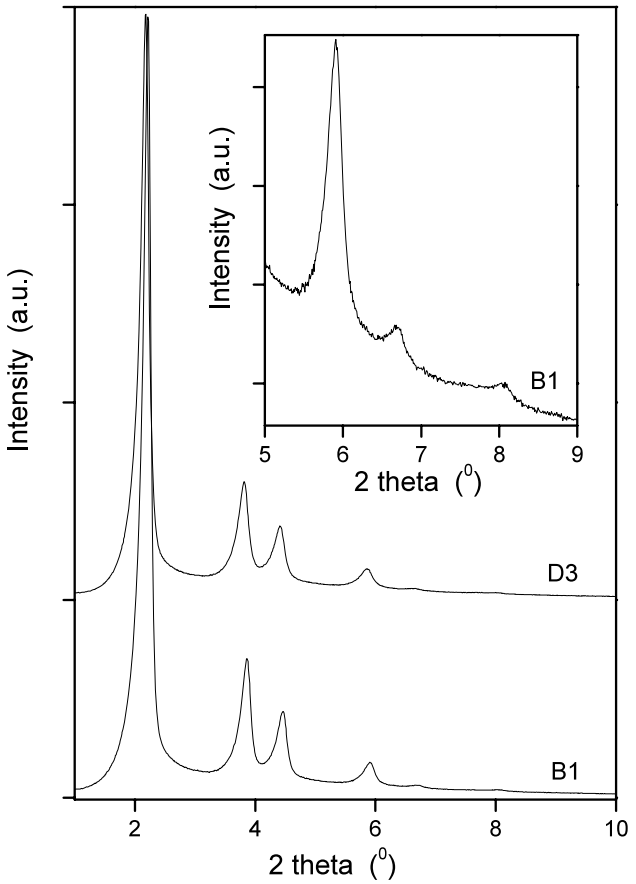

Fig. 6 XRD patterns of samples of series B1 and D3. The *inset* shows enlarged pattern of the sample B1

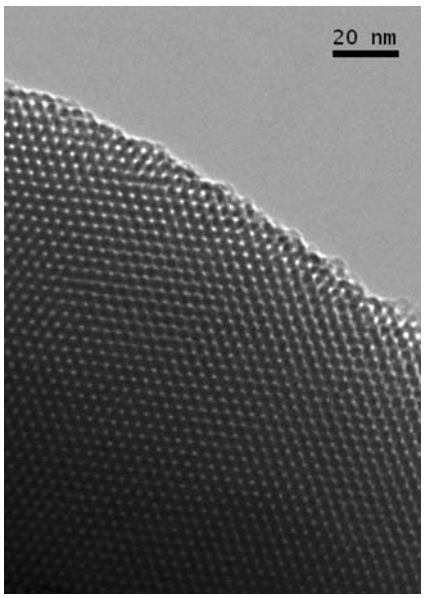

Fig. 7 HRTEM image of the sample A2 9 (a view across the pores)

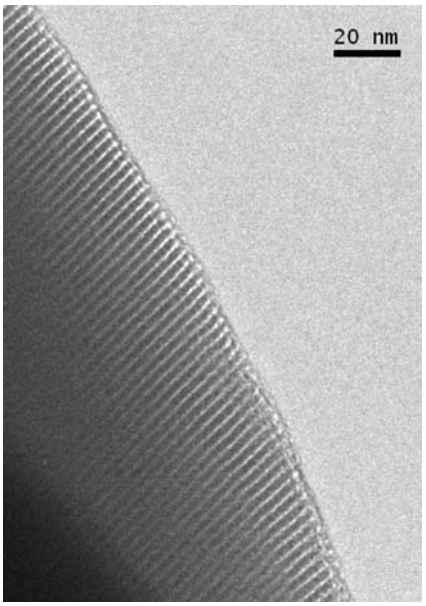

Fig. 8 HRTEM image of the sample A2 (a view along the pores)

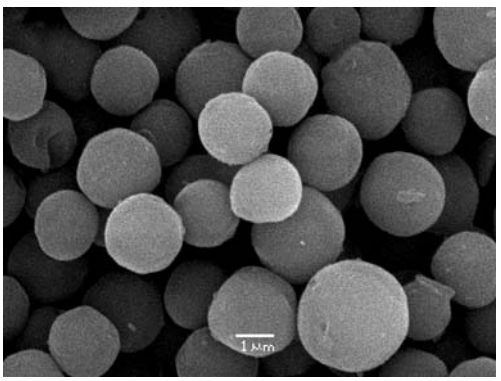

Fig. 9 SEM image of the sample A2

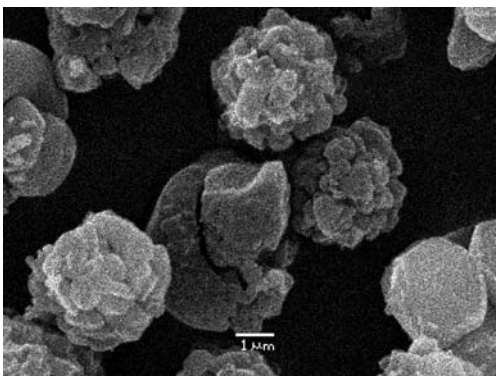

Fig. 10 SEM image of the sample B1

take place. As shown in Fig. 10, these particles have a tendency to agglomerate forming larger irregularly shaped agglomerates. Note, that the best samples B1 and D3 from series B, C, and D were prepared from the reaction mix-

tures containing the large amount of C_{16}MIMCl. With regard to this fact, the well-ordered mesoporous structure of these samples is believed to be a result of optimum or nearly optimum value of the packing factor g.

The spherical symmetry of particles of the sample A2 seems to be in contrast to 2D hexagonal ordering of mesopores. The possible explanation of this apparent contradiction can be based on the supposition that the rate of silica condensation in the course of mesophase formation is slower in comparison with the samples B1 and D3. In the early stages of the synthesis, the decrease in pH induces the formation of small mesophase particles. Due to the low rate of silica condensation these "liquid-like" particles aggregate to form larger particles, which are spherical in shape and consist of domains of perfectly ordered hexagonal structure. In the subsequent stages, the polymerization of silica leads to the "frozen" spherical particles. Due to the charge density matching these particles feature ordered hexagonal mesoporous structure.

4 Conclusion

A procedure for the synthesis of siliceous mesoporous molecular sieve MCM-41 based on the precipitation of the solid product from a homogeneous water solution of sodium metasilicate and the blends of 1-alkyl-3-methylimidazolium and alkyltrimethylammonium salts or blends of two different 1-alkyl-3-methylimidazolium salts was developed. All samples prepared were MCM-41 silicas characterized by the surface area of about 1000 m^2/g. The silica synthesized by using of the optimized blend of 1-octyl-3-methylimidazolium chloride and hexadecyltrimethylammonium bromide features the regular spherical particles with diameter of $\sim$2 μm. The characterization performed by means of scanning and high resolution electron microscopy, X-ray powder diffraction, and nitrogen adsorption has shown that the particles of this MCM-41 silica consist of domains of perfectly ordered mesoporous structure. The silicas prepared with optimized blends of 1-methyl-3-hexadecylimidazolium chloride and octyltrimethylammonium bromide or 1-methyl-3-octylimidazolium chloride and 1-methyl-3-hexadecylimidazolium chloride feature the perfectly ordered mesoporous structure with a small volume of secondary mesopores.

Acknowledgements A.Z. and J.Č. thank the European Community (SES6-CT-2005-020133) and the Academy of Sciences of the Czech Republic (KAN100400701) for a financial support of this study. H.Š. acknowledges the support of the Grant Agency of the Czech Republic (203/03/H0140). The authors also thank Dr. L. Brabec (J. Heyrovský Institute) for recording SEM images.

References

Adams, C.J., Bradley, A.E., Seddon, K.R.: The synthesis of mesoporous materials using novel ionic liquid templates in water. Aust. J. Chem. **54**, 679–691 (2001)

Antonietti, M., Kuang, D., Smarsly, B., Zhou, Y.: Ionic liquids for the convenient synthesis of functional nanoparticles and other inorganic nanostructures. Angew. Chem. Int. Ed. **43**, 4988–4992 (2004)

Chen, F., Huang, L., Li, Q.: Synthesis of MCM-48 using mixed cationic-anionic surfactants as templates. Chem. Mater. **9**, 2685–2686 (1997)

Chen, F., Yan, X., Li, Q.: Effect of hydrothermal conditions on the synthesis of siliceous MCM-48 in mixed cationic-anionic surfactants systems. Stud. Surf. Sci. Catal. **117**, 273–280 (1998)

Cheng, Y.-R., Lin, H.-P., Mou, C.-Y.: Control of mesostructure and morphology of surfactant-templated silica in a mixed surfactant system. Phys. Chem. Chem. Phys. **1**, 5051–5058 (1999)

Gordon, C.M.: New developments in catalysis using ionic liquids. Appl. Catal. A Gen. **222**, 101–117 (2001)

Khushalani, D., Kuperman, A., Coombs, N., Ozin, G.A.: Mixed surfactant assemblies in the synthesis of mesoporous silicas. Chem. Mater. **8**, 2188–2193 (1996)

Kim, J.M., Sakamoto, Y., Hwang, Y.K., Kwon, Y.-U., Terasaki, O., Park, S.-E., Stucky, G.D.: Structural design of mesoporous silica by micelle-packing control using blends of amphiphilic block copolymers. J. Phys. Chem. B **106**, 2552–2558 (2002)

Kim, T.-W., Ryoo, R., Kruk, M., Gierszal, K.P., Jaroniec, M., Kamiya, S., Terasaki, O.: Tailoring the pore structure of SBA-15 silica molecular sieve through the use of copolymer blends and control of synthesis temperature and time. J. Phys. Chem. B **108**, 11480–11489 (2004)

Kresge, C.T., Leonowicz, M.E., Roth, W.J., Vartuli, J.C., Beck, J.S.: Ordered mesoporous molecular sieves synthesized by a liquid-crystal template mechanism. Nature **359**, 710–712 (1992)

Kruk, M., Jaroniec, M., Sayari, A.: Application of large pore MCM-41 molecular sieves to improve pore size analysis using nitrogen adsorption measurements. Langmuir **13**, 6267–6273 (1997)

Lagrost, C., Carrié, D., Vaultier, M., Hapiot, P.: Reactivities of some electrogenerated organic cation radicals in room-temperature ionic liquids: toward an alternative to volatile organic solvents? J. Phys. Chem. A 745–752 (2003)

Lin, H.-P., Wong, S.-T., Mou, C.-Y., Tang, C.-Y.: Extensive void defects in mesoporous aluminosilicate MCM-41. J. Phys. Chem. B **104**, 8967–8975 (2000)

Lowell, S., Shields, J.E., Thomas, M.A., Thommes, M.: Characterization of Porous Solids and Powders: Surface Area, Pore Size and Density, pp. 33–34. Kluwer, Dordrecht (2004)

Miskolczy, Z., Sebök-Nagy, K., Biczók, L., Göktürk, S.: Aggregation and micelle formation of ionic liquids in aqueous solution. Chem. Phys. Lett. **400**, 296–300 (2004)

Monnier, A., Schüth, F., Huo, Q., Kumar, D., Margolese, D., Maxwell, R.S., Stucky, G.D., Krishnamurty, M., Petroff, O., Firouzi, A., Janicke, M., Chmelka, B.F.: Cooperative formation of inorganic-organic interfaces in the synthesis of silicate mesostructures. Science **261**, 1299–1303 (1993)

Neimark, A.V., Ravikovitch, P.I.: Capillary condensation in MMS and pore structure characterization. Microporous Mesoporous Mater. **44-45**, 697–707 (2001)

Rathouský, J., Zukal, A.: Generalized homogeneous precipitation method for precisely controlled synthesis of mesoporous silica. Stud. Surf. Sci. Catal. **146**, 185–188 (2003)

Rathouský, J., Zukalová, M., Kooyman, P.J., Zukal, A.: Synthesis and characterization of colloidal MCM-41. Colloids Surf. A **241**, 81–86 (2004)

Ravikovitch, P.I., Neimark, A.V.: Characterization of nanoporous materials from adsorption and desorption isotherms. Colloids Surf. A **187**, 11–21 (2001)

Roth, W.J., Vartuli, J.C.: Synthesis of mesoporous molecular sieves. Stud. Surf. Sci. Catal. **157**, 91–110 (2005)

Ryoo, R., Ko, C.H., Park, I.-S.: Synthesis of highly ordered CM-41 by micelle-packing control with mixed surfactants. Chem. Commun., 1413–1414 (1999a)

Ryoo, R., Joo, S.H., Kim, J.M.: Energetically favored formation of MCM-48 from cationic-neutral surfactants mixtures. J. Phys. Chem. B **103**, 7435–7440 (1999b)

Scurto, A.M., Aki, S.N.V.K., Brennecke, J.F.: Carbon dioxide induced separation of ionic liquids and water. Chem. Commun., 572–573 (2003)

Trewyn, B.G., Whitman, C.M., Lin, V.S.-Y.: Morphological control of room-temperature ionic liquid templated mesoporous silica nanoparticles for controlled release of antibacterial agents. Nano Lett. **4**, 2139–2143 (2004)

Wang, T., Kaper, H., Antonietti, M., Smarsly, B.: Templating behavior of a long-chain ionic liquid in the hydrothermal synthesis of mesoporous silica. Langmuir, in press

Wasserscheid, P., Keim, W.: Ionic liquids—new "solutions" for transition metal catalysis. Angew. Chem. Int. Ed. **39**, 3772–3789 (2000)

Wasserscheid, P., Welton, T. (eds.): Ionic Liquids in Synthesis. Wiley-VCH, Weinheim (2003)

Welton, T.: Room-temperature ionic liquids. Solvents for synthesis and catalysis. Chem. Rev. **99**, 2071–2084 (1999)

Zhou, Y., Antonietti, M.: Preparation of highly ordered monolithic super-microporous lamellar silica with a room-temperature ionic liquid as template via the nanocasting technique. Adv. Mater. **15**, 1452–1544 (2003)

Zhou, Y., Antonietti, M.: A series of highly ordered, super-microporous, lamellar silicas prepared by nanocasting with ionic liquids. Chem. Mater. **16**, 544–550 (2004)

Zhou, Y., Schattka, J.H., Antonietti, M.: Room-temperature ionic liquids as template to monolithic mesoporous silica with wormlike pores via a sol-gel nanocasting technique. Nano Lett. **4**, 477–481 (2004)

Zhu, K., Pozgan, F., D'Souza, L., Richards, R.M.: Ionic liquid templated high surface area mesoporous silica and Ru-SiO_2. Microporous Mesoporous Mater. **91**, 40–46 (2006)

Zukal, A., Thommes, M., Čejka, J.: Synthesis of highly ordered MCM-41 silica with spherical particles. Microporous Mesoporous Mater. **104**, 52–58 (2007)

Žilková, N., Zukal, A., Čejka, J.: Synthesis of organized mesoporous alumina templated with ionic liquids. Microporous Mesoporous Mater. **95**, 176–179 (2006)